Formation of Nematic Liquid Crystals in Suspensions of Hard Colloidal Platelets

Felix M. van der Kooij and Henk N. W. Lekkerkerker*

Van't Hoff Laboratory for Physical and Colloid Chemistry, Debye Institute, Utrecht University, Padualaan 8, 3584 CH Utrecht, The Netherlands

Received: March 17, 1998; In Final Form: June 2, 1998

A novel model system of hard colloidal platelets was observed to phase-separate into an isotropic and a liquid crystalline phase. Polarization microscopy revealed that the liquid crystalline phase was of nematic origin. With such orientational ordering in suspensions of platelike particles already being predicted in the 1940s by Onsager's theory and corroborated more recently by computer simulations, a direct comparison with experimental observations has now become possible. Furthermore, the apparently unhindered formation of a macroscopic nematic phase in a suspension of hard platelets sheds new light on the issue of gelation instead of nematic phase formation in suspensions of clay platelets.

Introduction

Compared to the crystal and glass transitions that are known for colloidal systems of hard (i.e., short-range repulsive) spheres,[1] the phase behavior of hard anisometric particles is much richer due to the possibility of orientational ordering.[2] It was shown by Onsager[3] that the thermodynamic stability of these liquid crystalline phases arises from a gain of translational entropy that overrules the loss of orientational entropy associated with particle alignment. Numerous investigations, starting with the classic work on vanadium pentoxide[4] and tobacco mosaic virus,[5,6] have confirmed the validity of Onsager's theory for suspensions of repulsive rodlike particles. But, as was pointed out already by Onsager himself, the entropy-driven formation of liquid crystals should not be restricted to rodlike particles but should also apply to particles of platelike shape. More recently this was confirmed by computer simulations.[7,8] These studies also showed that for an isotropic suspension of disks of not too low anisometry the first ordered phase to be observed upon increasing the concentration is the nematic phase, in which there exists orientational order without positional order. In the widely studied model system for colloidal platelets, aqueous suspensions of clay particles, a sol−gel transition turns out to be ubiquitous instead.[9−12] A few observations have been reported that indicate that some degree of ordering may exist in these clay gels. Birefringence, as observed between crossed polarizers[11,13] and by polarization microscopy,[11] suggests that alignment of clay platelets may occur on a small length scale. Macroscopic separation between such a birefringent phase and an isotropic phase almost always seems to be inhibited by the rigidity of the gel network.[9,11] In exceptional cases however, notably by Langmuir[14] in 1938, this separation did occur. In addition to the observation of birefringence, a peak in the structure factor has been found by small-angle neutron scattering and small-angle X-ray scattering on clay gels,[13,15−17] indicating the presence of a characteristic spacing between the platelets which is not to be expected for nematic ordering. Paradoxically, the same interactions between clay platelets in suspension that largely explain their widely spread use in technology apparently disqualify them as a simple model for platelike particles undergoing the isotropic to nematic phase transition. Clearly the study of liquid crystal phase transitions in suspensions of plates demands a novel system, consisting of particles with just short-range repulsive forces such as those described in Onsager's theory. It is such a system that we report on here.

Experimental Section

Synthesis. The novel model system for hard platelike colloids consists of sterically stabilized gibbsite platelets dispersed in toluene. The first step of its synthesis comprises the preparation of an aqueous suspension of gibbsite ($Al(OH)_3$) platelets, by autoclaving a 0.9 M HCl solution containing 0.8 M aluminum *sec*-butoxide and 0.8 M aluminum isopropoxide (all analytical grade) for 72 h at 85 °C.[18−20] After dialyzing the resulting suspension against deionized water for a week, the platelets were sterically stabilized analogous to the method of Buining et al. for grafting boehmite rods.[21] To 600 mL of the ±0.7% (w/w) dialyzed aqueous suspension 2 L of propanol (technical grade) was added under sonication (in 1 h). Water was removed by distillation while keeping the dispersion volume constant by adding propanol. A 25 g sample of the steric stabilizer, a $M_w \approx 1000$ modified polyisobutene with Shell code SAP230, dissolved in 2 L of THF (technical grade) was then added under sonication. Conveyance of the suspension to toluene was achieved by distillation while adding toluene (technical grade), starting with the addition of 500 mL when 1 L was distilled and keeping the volume constant when another 500 mL was removed. The excess amount of polymer was removed by a sequence of sedimentation (3 h, 10 000 rpm) and redispersioning in toluene (analytical grade), which was repeated three times.

Characterization. In good solvents, like in this case toluene, the grafted polymer layer acts as a steric stabilizer which should give rise to steeply repulsive particle interactions.[22] As a result, the dispersions exhibit long-term stability, and free-lying platelets are displayed by transmission electron microscopy (TEM) as shown in Figure 1. The diameter of the platelets was determined by interactive image analysis of TEM micrographs, as the diameter of a circle with an area equal to that of the measured particle. To the number average following from this measurement the thickness of the polymer layer (4 nm)

* Fax: +31-302533870. E-mail: H.N.W.Lekkerkerker@chem.uu.nl.

S1089-5647(98)01534-X CCC: $15.00
Published on Web 10/01/1998

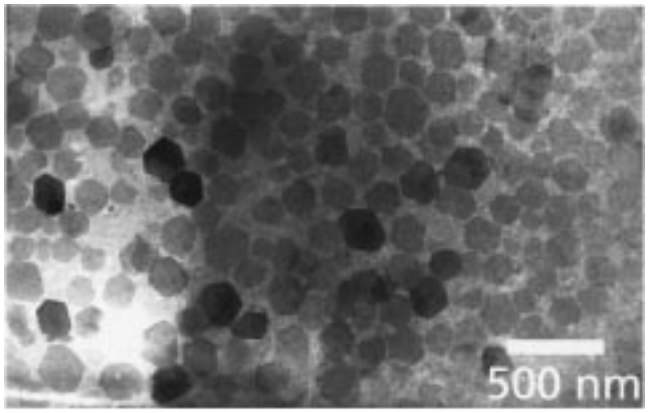

Figure 1. Transmission electron microscope (TEM) micrograph of the grafted gibbsite ($Al(OH)_3$) platelets.

was added twice to obtain the average diameter $\langle D \rangle$ of the grafted platelets, which was found to be 168 nm. The standard deviation $\sigma = \sqrt{\langle D^2 \rangle - \langle D \rangle^2}/\langle D \rangle = 0.25$ reflects the polydispersity of the platelet diameter. Likewise, twice the thickness of the polymer layer was added to the average thickness of the gibbsite platelets (as determined from the broadening of the X-ray (002) diffraction peak using the Scherrer equation), yielding an average total thickness $\langle L \rangle$ of 15 nm. Hence the aspect ratio $\langle D \rangle / \langle L \rangle$ of the grafted platelets is approximately 11. Volume fractions were calculated as the solid mass concentration of the dispersion, determined by drying a known amount of dispersion at 75 °C to constant weight, divided by the effective particle density including the solvent immobilized in the polymer layer.

Phase Separation Experiments. Raising and lowering of the volume fraction of platelets was achieved respectively by sedimentation in a table centrifuge followed by removal of solvent and dilution. Using a Zeiss Axioplan polarization microscope, the microscopic phase separation process was studied for samples with concentrations in the biphasic region which were inserted between a hollow glass slide and cover slip. The macroscopic behavior was studied for volume fractions up to 25%. Samples were thoroughly homogenized before being stored in a thermostated room for 2 days in order to be able to reach equilibrium.

Results

Upon raising the volume fraction of the dispersion above some threshold value, the first sign of the incipient phase transition was the persistence of birefringence after shaking the tube. Observations by polarization microscopy of such samples (Figure 2) indicate that the subsequent phase separation process involves the nucleation and growth of nematic droplets, which finally coalesce into Schlieren patterns that are characteristic for a nematic phase. Macroscopic observations of the dispersions are depicted in Figure 3. Up to 15.9% (v/v) samples remain isotropic throughout. Above 17.3% (v/v) rearrangement of shear-induced birefringence leads to a permanently birefringent nematic phase filling the entire dispersion volume. Between 15.9 and 17.3% (v/v), the sedimentation of small nematic droplets leads within 6 h to separation in an isotropic bottom phase and a permanently birefringent nematic upper phase, divided by a sharp boundary. In this biphasic gap the relative volume of the nematic phase increases almost linearly with the particle concentration (Figure 4). Repartitioning of the particle size distribution due to the phase separation was shown by TEM micrographs of the coexisting upper and lower phase to be insignificant.

Discussion

With experimental values for the isotropic−nematic transition densities now being available, a comparison with results obtained by calculations and computer simulations seems obvious. For the purpose of universality, transition densities can be expressed as dimensionless densities $n_{iso}D^3$ and $n_{nem}D^3$, where n_{iso} and n_{nem} denote the number density in the coexisting isotropic and nematic phase, respectively, and D is the diameter of the plates. Numerical solutions of the Onsager formalism

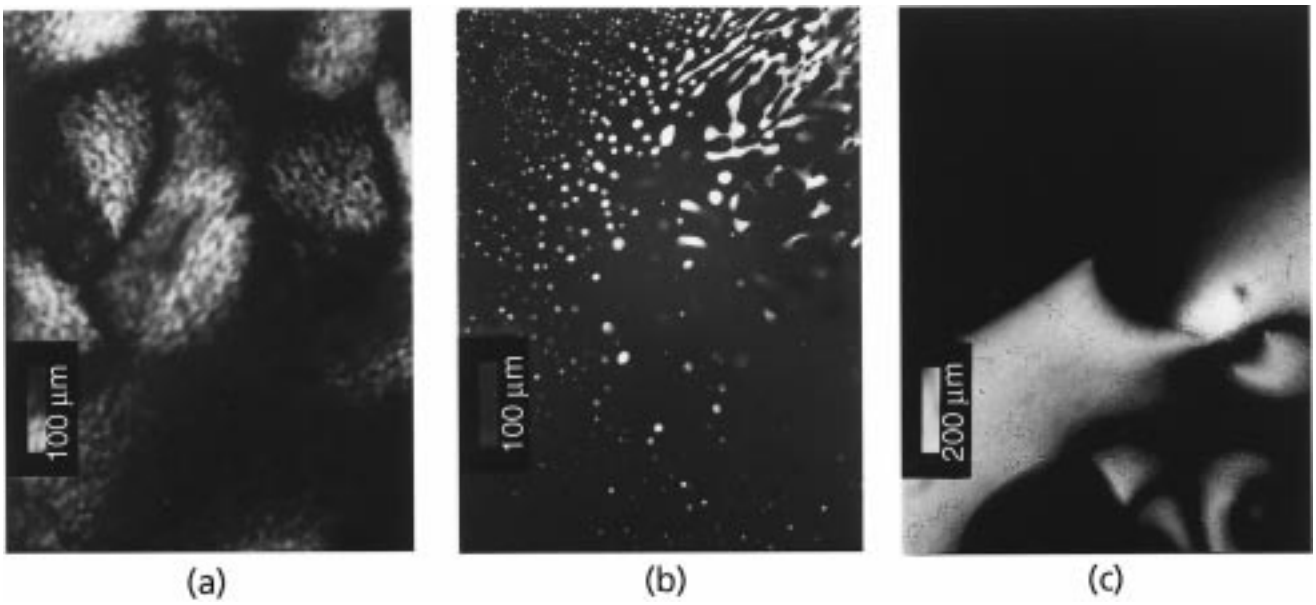

Figure 2. Microscopic observations between crossed polarizers of the phase separation process. (a) During the first 30 min, initial shear-induced regions of birefringence can be observed. (b) Nucleation and growth of nematic droplets (tactoids) lead to the breaking up of the shear-induced structure. Unlike phase-separating dispersions of rodlike particles, in which the observed tactoids are of spindlelike shape, tactoids formed by platelike particles seem to possess a more rounded shape. This phenomenon is likely to be associated with the different morphology of the particles. (c) Nematic Schlieren pattern formed after a few hours, when the phase separation is complete.

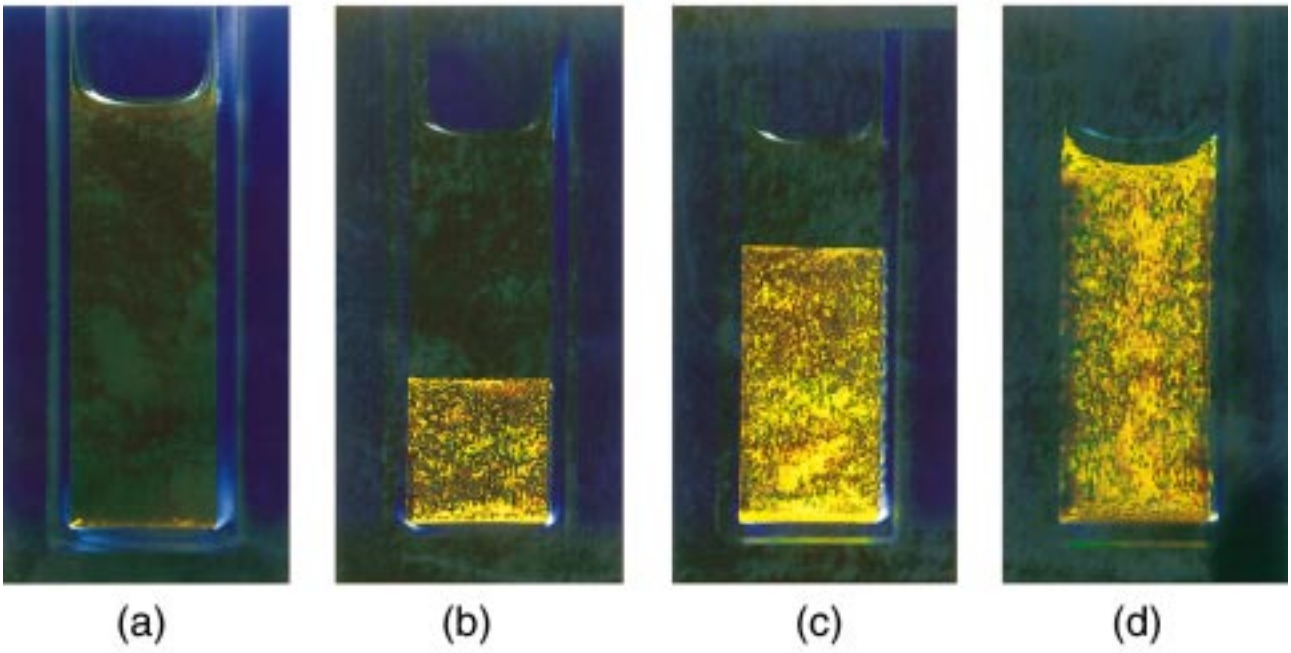

Figure 3. Isotropic−nematic phase separation as observed between crossed polarizers, at volume fractions ranging from (a) 15.9, (b) 16.5, (c) 16.9, to (d) 17.4% (v/v). The isotropic upper phase shows streaming birefringence when the tube is slightly shaken, indicating the presence of free alignable platelets. The lower phase is permanently birefringent due to nematic ordering and shows its liquid crystalline nature by flowing like a moderately viscous liquid when the tube is tilted.

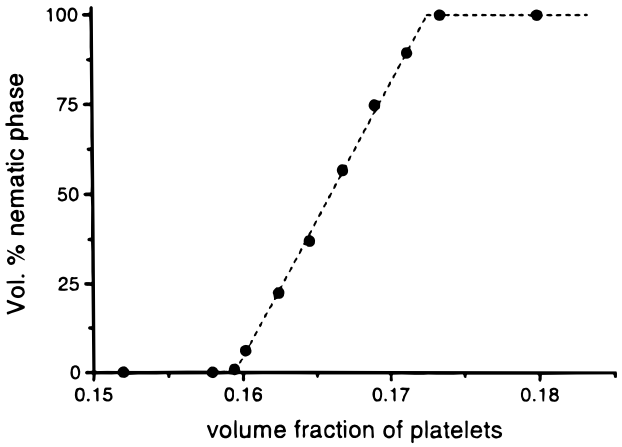

Figure 4. Volume of the nematic phase relative to the total dispersion volume, plotted as a function of the volume fraction of the platelets.

directly applied to disks were found by Forsyth et al.[23,24] They obtained $n_{iso}D^3 = 6.8$ and $n_{nem}D^3 = 7.7$ for the coexisting isotropic and nematic phases for disks with an aspect ratio of 10. In the limit of infinitely thin disks, $n_{iso}D^3$ and $n_{nem}D^3$ were observed to decrease to 5.3 and 6.8, respectively. But, as was already pointed out by Onsager,[3] applying the formalism to disks inevitably leads to erroneous transition densities because truncation of the virial equation of state after B_2 may be justified for long rods but not for disks. In a Monte Carlo (MC) simulation that does include virial coefficients up to the fifth, Eppenga and Frenkel[7] found $n_{iso}D^3$ and $n_{nem}D^3$ for infinitely thin disks to be 4.04 and 4.12, respectively. The effect of reducing the aspect ratio to 10 was found to be limited in a similar MC study by Veerman and Frenkel,[8] which yielded $n_{iso}D^3 = 3.81$ and $n_{nem}D^3 = 3.87$. Because of the accuracy of the five-term virial series and the resemblance with the value of 11 for the aspect ratio of the experimental system, the latter study seems to be the most relevant for means of comparison with our experiment. Bearing in mind that our experimental system is not monodisperse, experimental volume fractions of platelets can be converted to number densities according to $\phi/[(\pi/4)\langle D^2\rangle\langle L\rangle]$, assuming D and L to be uncorrelated. Expressing in terms of the dimensionless densities, and using the binomial expansion for a narrow distribution,[25] one obtains

$$n\langle D^3\rangle = \frac{4}{\pi}\phi\frac{\langle D^3\rangle}{\langle D^2\rangle\langle L\rangle} = \frac{4}{\pi}\phi\frac{(1+3\sigma^2)\langle D\rangle^3}{(1+\sigma^2)\langle D\rangle^2\langle L\rangle} = \frac{4}{\pi}\phi\frac{(1+3\sigma^2)\langle D\rangle}{(1+\sigma^2)\langle L\rangle}$$

Inserting into this equation the value of 11 for the aspect ratio of the platelets, the standard deviation in diameter, and the experimentally determined volume fractions at which the transition occurs yields the dimensionless transition densities $n_{iso}\langle D^3\rangle = 2.5$ and $n_{nem}\langle D^3\rangle = 2.7$. Several contributions can be distinguished that may explain the discrepancy between theoretical and experimental transition densities. From the much better investigated class of liquid crystals in suspensions of rodlike particles, polydispersity is known to shift the biphasic region to lower density as well as broaden it in a significant way.[22,26] Also shape details, i.e., the use of hexagons instead of disks, and possibly a slight attraction between the platelets may play a role.

Let us now return to the case of suspensions of clay platelets, for which, unlike the hard plates considered in this study, the isotropic−nematic phase coexistence seems so hard to reach. The main difference with the hard plate system lies in the nature of the interparticle interaction, which in the case of clay platelets is based on charge stabilization. As it determines the double layer extension, the ionic strength of the suspension will have a major effect on the effective degree of anisometry, the apparent particle volume, the suspension viscosity, and even the sign of the interparticle interaction. There is no doubt that these interrelated parameters will determine not only the thermodynamically most stable phase at that concentration but also the kinetics of any structural change in the suspension. While for

charge-stabilized suspensions of rods such as tobacco mosaic virus, vanadium pentoxide, and boehmite the phase diagram has indeed been observed to include an I−N phase coexistence region, the paucity of experimental observations of I−N coexistence for charged plates suggests that fine-tuning of the ionic-strength-related parameters is more delicate in the case of plates. The present contribution to this subject is to elucidate that for the special case of simple hard plates an isotropic to nematic phase transition indeed occurs in an experiment, at transition densities that are somewhat lower than those predicted by simulations.

Acknowledgment. We thank professors A. P. Philipse and D. Frenkel for helpful discussions. This work was supported by the Foundation for Fundamental Research on Matter (FOM), which is part of The Netherlands Organization for the Advancement of Research (NWO).

References and Notes

(1) Pusey, P. N.; van Megen, W. *Nature* **1986**, *320*, 340.
(2) Vroege, G. J.; Lekkerkerker, H. N. W. *Rep. Prog. Phys.* **1992**, *55*, 1241.
(3) Onsager, L. *Ann. N. Y. Acad. Sci.* **1949**, *51*, 627.
(4) Zocher, H. *Anorg. Allg. Chem.* **1925**, *147*, 91.
(5) Bernal, J. D.; Fankuchen, I. *J. Gen. Physiol.* **1941**, *25*, 111.
(6) Oster, G. *J. Gen. Physiol.* **1950**, *33*, 445.
(7) Eppenga, R.; Frenkel, D. *Mol. Phys.* **1984**, *52*, 1303.
(8) Veerman, J. A. C.; Frenkel, D. *Phys. Rev. A* **1992**, *45*, 5632.
(9) Mourchid, A.; Delville, A.; Lambard, J.; Lecolier, E.; Levitz, P. *Langmuir* **1995**, *11*, 1942.
(10) Dijkstra, M.; Hansen, J.-P.; Madden, P. A. *Phys. Rev. E* **1996**, *55*, 3044.
(11) Gabriel, J.-C. P.; Sanchez, C.; Davidson, P. *J. Phys. Chem.* **1996**, *100*, 11139.
(12) Callaghan, I. C.; Ottewil, R. H. *Faraday Discuss. Chem. Soc.* **1974**, *57*, 110.
(13) Yamaguchi, Y. Investigation of a synthetic clay mineral (saponite) in aqueous solution and surfactant mixtures, Dissertation, Bayreuth University, 1997.
(14) Langmuir, I. *J. Chem. Phys.* **1938**, *6*, 873.
(15) Ramsay, J. D. F.; Swanton, S. W.; Bunce, J. *J. Chem. Soc., Faraday Trans.* **1990**, *86*, 3919.
(16) Ramsay, J. D. F.; Lindner, P. *J. Chem. Soc., Faraday Trans.* **1993**, *89*, 4207.
(17) Morvan, M.; Espinat, D.; Lambard, J.; Zemb, T. *Colloids Surf. A* **1994**, *82*, 193.
(18) Buining, P. A.; Patmamanoharan, C.; Jansen, J. B. H.; Lekkerkerker, H. N. W. *J. Am. Ceram. Soc.* **1991**, *76*, 1303.
(19) Philipse, A. P.; Nechifor, A. M.; Patmamanoharan, C. *Langmuir* **1994**, *10*, 4451.
(20) Wierenga, A.; Lenstra, T. A. J.; Philipse, A. P. *Colloids Surf. A* **1997**, *134*, 359.
(21) Buining, P. A.; Veldhuizen, Y. S. J.; Patmamanoharan, C.; Lekkerkerker, H. N. W. *Colloids Surf.* **1992**, *64*, 47.
(22) Buining, P. A.; Lekkerkerker, H. N. W. *J. Phys. Chem.* **1993**, *97*, 11510.
(23) Forsyth, P. A.; Marcelja, S.; Mitchell, D. J.; Ninham, B. W. *J. Chem. Soc., Faraday Trans. 2* **1977**, *73*, 84.
(24) Forsyth, P. A.; Marcelja, J. S.; Mitchell, D. J.; Ninham, B. W. *Adv. Colloid Interface Sci.* **1978**, *9*, 37.
(25) Pusey, P. N.; Fijnaut, H. M.; Vrij, A. *J. Chem. Phys.* **1982**, *77*, 4270.
(26) Vroege, G. J.; Lekkerkerker, H. N. W. *J. Phys. Chem.* **1993**, *97*, 3601.